Environmental Engineering and Management Journal

October 2023, Vol. 22, No. 10, 1689-1702
http://www.eemj.icpm.tuiasi.ro/; http://www.eemj.eu
http://doi.org/10.30638/eemj.2023.144

"Gheorghe Asachi" Technical University of Iasi, Romania

CO-HYDROTHERMAL CARBONIZATION OF CAVITATED STABILIZED ORGANIC FRACTION AND LANDFILL LEACHATE: OPTIMIZATION OF HYDROCHAR CHARACTERISTICS

Alessandro Cardarelli[1]*, Pierpaolo Lombardi[2], Andrea Nicolini[3], Marco Barbanera[1]

[1]Department of Economics Engineering Society and Business Organization (DEIM), University of Tuscia, Largo dell'Università s.n.c., Loc. Riello, 01100 Viterbo, Italy
[2]Ecologia Viterbo srl, Via Atto Tigri, 11, 00197, Roma, Italy
[3]CIRIAF (Inter-University Research Center on Pollution and Environment "Mauro Felli"), Biomass Research Centre, University of Perugia, Perugia, Italy

Abstract

The problem of municipal solid waste (MSW) management is becoming an issue more and more relevant. Hydrothermal carbonization (HTC) is an emerging path to address the concerns arising from the management of MSW, promoting a from-waste-to-resource action plan. In this study, the HTC was performed by using the stabilized organic fraction (SOF) of the MSW to evaluate the hydrochar characteristics and to determine the optimum temperature and residence time of the HTC process. Preliminary tests were achieved with SOF and two different liquid substrates, the landfill leachate (LL) and the concentrate fraction (CF) of landfill leachate from the reverse osmosis plant, respectively. The HTC was performed at different process temperatures and residence times, while the solid-to-liquid ratio was maintained at 1/10. Furthermore, the influence of hydrodynamic cavitation (HC) to enhance the homogenization of SOF and liquid substrate before the HTC was studied. Response Surface Methodology (RSM) was applied to determine the best HTC process conditions (process temperature and residence time) based on the experimental campaign developed through the Central Composite Face-Centered Design (CCF-CD). By statistical analysis, it was possible to understand how the process variables influenced the fixed carbon content, deashing efficiency and mass yield (considered as responses of the model). The optimum condition for the HTC process was at 232°C and 2.65 h. The preliminary results showed that the hydrochar from HTC of the cavitated blend of SOF and LL is a valid mixture for the production of eco-sustainable plasters to be used in the building sector in a circular economy approach.

Key words: HTC, hydrochar, hydrodynamic cavitation, municipal solid waste, response surface methodology

Received: May, 2023; Revised final: July, 2023; Accepted: August, 2023; Published in final edited form: October, 2023

1. Introduction

Approximately 232 million tonnes of municipal solid waste, or 517 kg per capita, were produced in 2020 in the UE27. In the three years 2018–2020, there was an increase of 3.7% in production overall (Eurostat, 2023). In 2021, in Italy, the production of municipal waste involved a quantity of about 30 million tons, the solution of which final mainly involves landfilling. Such a solution not only occupies more and more valuable space but also causes air, water and soil pollution by discharging carbon dioxide carbon (CO_2) and methane (CH_4) into the atmosphere and chemicals and pesticides in the land and the groundwater. This, in turn, is harmful to human health, as well as the environment.

Mechanical Biological Treatment (MBT) is widely used as a form of pretreatment to landfill or incineration. It is an essential phase of the waste cycle since allows, through a process of selection (mechanical) and treatment (biological), to:

- recover a further part of recyclable materials;

* Author to whom all correspondence should be addressed: e-mail: a.cardarelli@unitus.it

- make an appropriate selection of waste to be sent for incineration/waste-to-energy plant, obtaining a lower emission of pollutants and a higher energy yield;
- reduce the volume of material for final disposal and therefore the use of landfills and incinerators;
- ensure the conditions of biological stability of the waste to minimise the formation of decomposition gases and leachate.

In an MBT plant, the unsorted MSW is mechanically sorted into three fractions, i.e. material organic, recyclables and waste. The recyclable fraction includes materials such as glass, metals, plastics, rubber, rags, papers etc. which can be differentiated by separation and sieving. The recyclable components (glass, metals etc.) can be sent for recycling, while the components non-recyclable partly contribute to the production of solid fuel to be sent to waste-to-energy plants and parts are sent to landfill.

The organic fraction is addressed to a biological stabilization process (aerobic digestion). The output of the aerobic digestion is called stabilized organic fraction (SOF), or off-specification compost, and it is codified by the European Waste Catalog (EWC) as EWC 19.05.03. This material is currently discarded and landfilled, with additional costs. According to the Urban Waste Report 2022 of ISPRA (ISPRA, 2022), in 2021 over 8.1 million tons of waste/materials were produced by mechanical biological treatment plants, which is about 560.000 tons of SOF. Furthermore, leachate is generated from the MSW landfilling. Landfill leachate (LL) is a tainted liquid arising from the bottom of solid waste disposal facilities that contain both soluble organic and inorganic compounds as well as suspended particles (Naveen et al., 2017).

In Italy, the regulation requires that it must be captured and appropriately treated on the same site of the landfill or transported in an ad hoc plant duly authorized for disposal in the sewers. Currently, physicochemical treatment methods such as reverse osmosis are widely used. Reverse osmosis membrane technology plants are employed for LL treatment, producing two fractions: the permeate (PF) (about 75%) and the concentrate (CF) (about 25%). Since the permeate might be directed to the sewers, the concentrate remains a burden. In this context, alternatives are needed to valorize the SOF, together with landfill waste reduction, as well as the landfill leachate and/or concentrate, leading the waste management business towards a circular economy perspective.

A valuable option is to use all these wastes as precursors in the production of carbon-based materials. This work arises from the project ECOPLASTER - Biostabilized for Ecosustainable Building -funded in 2022 by the Ministry of Environment and Energetic Security. The project intends to use the outputs of the municipal solid waste management chain, i.e. SOF, LL, and the CF as input for the hydrothermal carbonization (HTC) process. The HTC is a thermochemical valorization process during which the wet biomass remains heated at a low temperature range (150–350°C) over a few minutes to several hours under autogenic pressure (Villamil et al., 2020). Three types of products are resulting from the process. The main output is a carbon-rich solid material known as hydrochar, which accounts for approximately 45-70% of the product mass. A gas phase, approximately 1-3% of the raw material, consisting mainly of CO_2 (>90% of the gaseous products) with small amounts of CH_4, H_2, and CO. A liquid fraction (spent liquor), 5 and 25% of the mass of products, which is rich in bio-degradable soluble organic compounds (Magdziarz et al., 2021; Roman et al., 2021; Wilk et al., 2020). The HTC process has several advantages, including the ability to process heterogeneous wet biomasses without pre-drying or separation pre-treatment required by other thermochemical processes, since water acts as a reactant, solvent, and catalyst (Libra et al., 2011; Sharma et al., 2020). These advantages make the HTC process applicable to various wet residues, including agricultural and forestry residues (Başakçılardan Kabakcı and Baran, 2019), anaerobic digestate (Cavali et al., 2023), sewage sludge (Luo et al., 2020), algal biomass (Castro et al., 2021; Jabeen et al., 2023), olive mill sludge (Mendecka et al., 2020), pulp and paper mill sludge (Mohammadi et al., 2020) and off-specification compost (Basso et al., 2015). Nonetheless, within the HTC process, there are present some disadvantages. These include the use of complex and costly systems which use substantial amounts of water and further costs for the separation of the solid and liquid phases, as well as the discharge of significant quantities of wastewater (Ercan et al., 2023; Khan et al., 2019).

However, current research examining the possible valorization of the spent liquor derived from the biomass HTC process highlights the commercial rentability in a circular economy approach (Khan et al., 2019). Possible solutions cited include processes from which the resultant by-product represents a benefit such as anaerobic digestion, nutrient recovery, bioplastic production, wet oxidation, and liquid fertilizer (González-Arias et al., 2023; Ipiales et al., 2021; Langone and Basso, 2020; Tripathi et al., 2022; Zhang et al., 2023).

In the project ECOPLASTER, the hydrochar (solid fraction) of the HTC process will be used for the production of an eco-sustainable plaster to be used in the building sector, while the spent liquor (liquid fraction) will be employed for the growth of microorganisms aimed at the production of bioplastics. This study provides preliminary results on the application of the HTC process to the stabilized organic fraction of MSW for hydrochar production, by using both landfill leachate and the concentrate fraction as liquid substrate. Several studies have investigated the HTC as thermal pre-treatment for different types of MSWs, or streams obtained from it. (Ischia et al., 2021) performed the HTC to valorize

municipal solid waste for biofuel production; the off-specification compost was used by (González-Arias et al., 2021) to be co-processed by HTC with olive tree pruning and obtaining a coal-like product with a high carbon content; Periyavaram et al. (2023) analyzed the thermal behavior of hydrochar derived from HTC of food waste using leachate as moisture source; likewise, Śliz et al. (2022) reported the technical feasibility of an industrial scale layout of an HTC plant by using the wet fraction mechanically separated from mixed MSW or under sieve fraction as solid substrate and water as moisture source.

Despite the many probable benefits, the potential application of LL or CF from reverse osmosis plants as liquid substrates for HTC remains less explored. This study aimed at comparatively evaluating the efficacy of landfill leachate and concentrate fraction as reaction media for the hydrothermal conversion of SOF derived from MSWs to hydrochar.

Product yield and proximate and ultimate analyses were taken into consideration to understand the basic physicochemical properties of the resulting hydrochars and optimize the process parameters (residence time and temperature) of the hydrothermal carbonization to be used in an industrial scale-up. Moreover, to further enhance the homogenization and viscosity of the solid and liquid substrate mixture before the HTC process, the application of hydrodynamic cavitation (HC) was investigated. HC is a promising physicochemical process consisting of the phenomenon of formation, growth, and rapid collapse of vapor cavities due to the reduced local pressure (Lanfranchi et al., 2022). The HTC was carried out at different process temperatures and residence times, while the solid-to-liquid ratio was maintained constant. Furthermore, HC was performed at a temperature set point of 60°C in order to investigate its influence on the hydrochar physical-chemical characteristics.

Central Composite Face-Centered Design (CCF-CD) and Response Surface Methodology (RSM) were used to examine any potential relationships of the hydrochar production parameters (temperature and residence time) on the fixed carbon content (FC), deashing (DE) and mass yield (MY) of the hydrochars. In detail, FC, DE and MY were selected as response variables in the optimization process in order to obtain the HTC conditions at which the hydrochar characteristics were maximized to improve the efficiency of the admixture material to be used as plaster in the building sector for carbon-capture (Gupta and Kua, 2017; Navaratnam et al., 2021), moisture absorption (Mrad and Chehab, 2019) and thermal and acoustic insulation (Kahandawa Arachchi et al., 2021; Srikanth et al., 2022). The results of the present work will be used to define the optimal mixture of mortar and hydrochar for the production of eco-sustainable plasters to be employed in the building sector.

2. Material and methods

2.1. Collection of SOF and liquid substrates

The stabilized organic fraction, the landfill leachate, and the concentrate fraction of the reverse osmosis of LL were obtained from the same MSWs management plant located in Viterbo, Italy. The SOF was collected from the MBT and locally sieved down to a particle size of approximately 2.5 mm before the laboratory experiments in order to remove any inorganic residues, e.g. glass, metal, plastic, paper, etc. The LL was spilled from the MSW landfill while the CF came from the reverse osmosis plant, both located in the same area as the MBT plant. The LL and CF were gathered in plastic containers and stored at a temperature of +4°C. The characteristics in terms of pH, biochemical oxygen demand (BOD), chemical oxygen demand (COD), conductivity, and total solids (TS) at 105°C of each liquid substrate are listed in Table 1.

Table 1. Characteristics of each liquid substrate

Liquid substrate	***LL***	***CF***
pH	7.9	6.8
BOD [mg/L]	2150	638
COD [mg/L]	8380	2490
Conductivity [mS/cm]	25.6	23.7
Total solids [%]	2.0	1.4

2.2. HTC experiment

A stainless-steel Parr 4560 mini-batch reactor with a volume of 600 ml was used for the hydrothermal carbonization treatment. The removable ceramic band heater was connected to the external control system (4848 reactor controller, Parr Instrument) which allowed the setting of both the temperature and the rotational speed of the stirrer. For each experimental run, the vessel was loaded with the solid and liquid substrate and purged with nitrogen to remove the air from the reactor. The reactor was heated up to the desired temperature with a heating rate of 3°C/min while the stirring rate was set to 200 rpm. The residence time is referred to the holding time of the reactor after reaching the temperature set point. Then, the internal cooling coil connected with an external chiller allowed for an immediate decrease in temperature by the coolant. Thus, the liquor was separated by using a Büchner funnel with a vacuum pump and filter paper (Whatman filter paper, 8 μm). While the hydrochar was washed with distilled water several times and oven-dried at 105°C for 24 h to remove residual moisture, the liquid fraction was collected and maintained at +4°C for further analyses. The mass yield (*MY*) of the HTC process was calculated as the ratio of the mass of hydrochar (M_f) to that of the initial feedstock (M_0) on a dry basis by using Eq. (1).

$$MY = \frac{M_f}{M_0} * 100\ [\%] \quad (1)$$

2.3. Hydrodynamic cavitation

When the HTC process is scaled up to industrial size, the homogenization and viscosity of the solid and liquid substrate mixture become essential parameters affecting its pumpability. The pumpability of the slurry is limited by the type of pump, which generally have an upper limit of about 10-15% solids (dry basis) loading (Nagarajan and Ranade, 2021). Thus, hydrodynamic cavitation was selected as a pre-treatment to enhance these characteristics.

The HC was performed by using single-step homogenization with a controlled cavitation approach patented by SOLDO Cavitators (Soldo Cavitators, 2023). The cavitation unit is composed of a feed tank and a 5.5 kW electric motor which provides power to a stainless steel rotor (cavitator) working at 20 L/min, 3 bar, and 3600 rpm. The solid and liquid substrates were mixed at the desired solid-to-liquid ratio and pumped inside the cavitator in a closed loop until the flow temperature reached the set point of 60 °C.

2.4. Chemical-physical analysis

Proximate analysis was carried out following the standards EN 14774-2 for the moisture content, EN 15148 for the volatile matter (VM), and EN 14775 for the ash content, by using a thermogravimetric analyzer (TGA-701, LECO Co., USA). Ultimate analysis was performed by using a LECO Truspec CHN analyzer, in compliance with UNI EN 15104 standard method. Fixed carbon (FC) and oxygen were computed by difference. Moreover, the deashing efficiency (DE) of the HTC process was evaluated according to Eq. (2):

$$DE = \frac{Ash_{SOF} - (Ash_{Hydrochar,i} * MY_i)}{Ash_{SOF}} * 100\ [\%] \quad (2)$$

where Ash_{SOF} is the ash content of the stabilized organic fraction before the HTC treatment, $Ash_{Hydrochar,i}$ is the ash content of the hydrochar obtained from the HTC process regarding the i-th test. All measurements were conducted in triplicate and a mean value was reported. Furthermore, the specific surface area of the samples was examined with a BET analyzer (ASAP2460, Micromeritics, USA).

2.5. Preliminary tests and experimental design

Firstly, preliminary tests of HTC were conducted to understand the influence of the liquid substrate (landfill leachate and concentrate fraction) on the chemical properties of the hydrochar. The HTC was performed at different process temperatures (200, 250, and 270 °C) and residence times (1, 3, and 6 h), while the solid-to-liquid ratio was maintained at 1/10. Then, the effect of the hydrodynamic cavitation on the chemical characteristics of the hydrochar was evaluated by considering a temperature set point of 60°C. Response Surface Methodology (RSM) and Central Composite Face-Centered Design (CCF-CD) were used to examine any potential relationships between the hydrochar production parameters (temperature and residence time) and the impacts on the fixed carbon content, deashing, and mass yield. A three-level, 2-factor CCF-CD was employed. HTC process temperature (X_1) and residence time (X_2) were assumed as independent variables and coded at three levels (−1, 0, and +1), corresponding to the minimum, medium and maximum levels. Each process factor level was carefully selected based on preliminary tests. For the hydrochars, the chosen responses were fixed carbon content (Y_1), deashing efficiency (Y_2), and mass yield (Y_3) of the HTC process. The software Minitab v17.1.0 (Minitab Ltd., Coventry, UK) was used to implement the statistical model. The statistical significance of the regression coefficients was examined by using analysis of variance (ANOVA) and regression analysis. This was accomplished by using the Fisher's F-test at a 95% confidence level, following the methodology outlined by Buratti et al. (2018). Multi-response analysis, based on Derringer's desirability function, was used to concurrently optimize the response variables (Derringer and Suich, 1980). The desired response of FC content, DE, and MY was the maximum of the target goal. The same importance was assumed for each response during the optimization analysis.

The method is described more exhaustively by Barbanera et al. (2018). Three replications of experiments under optimum conditions were conducted to validate the optimized models by comparing the experimental data to the expected values.

3. Results and discussion

3.1. Characterization of preliminary tests

The characteristics of biomass before and after the HTC process in terms of proximate and ultimate analysis, mass yield, and deashing efficiency are shown in Table 2.

Preliminary results indicate that tests performed at 250°C and a residence time of 3 h with LL rather than CF produce hydrochar with improved characteristics. Dehydration, decarboxylation, hydrolysis, and condensation are the main reactions that occur during the hydrothermal carbonization process (Nawaz and Kumar, 2023; Wang et al., 2022a). The balance between these different reactions determines the carbon content of the resulting hydrochar. At moderate temperatures (250 °C) and residence times (3 hours), the HTC process primarily involves dehydration and decarboxylation reactions, which lead to an increase in the carbon content (Djandja et al., 2023), resulting in about +22% and 23% by using LL and CF respectively. However, as the reaction temperature and residence time increase (270°C and 6 hours), hydrolysis and condensation reactions become more prevalent, leading to a

decrease in the carbon content (Danso-Boateng et al., 2022) of about –5% and –21% by using LL and CF respectively. Thus, at lower temperatures and residence times, the increase in carbon content due to dehydration and decarboxylation reactions outweighs the decrease due to hydrolysis and condensation reactions. However, at higher temperatures and longer residence times, the decrease in carbon content due to hydrolysis and condensation reactions outperforms the increase due to dehydration and decarboxylation reactions, resulting in a net decrease in carbon content. Furthermore, for both the hydrochar obtained with LL and CF the ash content increased first and then lightly decreased as the temperature and residence time increased. A similar trend was found in literature (Chen et al., 2021). The reason might be attributed to the decrease of the organic compounds while the ash increased with the increment of the reaction temperature and residence time from 220 °C and 1 hour to 250 °C and 3 hours. However, with the further increase of the HTC process parameters (270 °C and 6 hours), the degradation of organic components promotes the decomposition of inorganics into the liquid fraction. Thus, despite a higher carbon content (+14.15%), the HTC of SOF with concentrate fraction promotes the formation of ashes (+7.19%) in comparison to using landfill leachate. Furthermore, by using the CF the deashing efficiency of the process resulted in a reduction of –51.69%. Higher ash content in hydrochar reduces its porosity as the inorganic materials can fill up the pore spaces. Additionally, ash could also coat the surface of hydrochar particles and reduce their specific area available for reactions or adsorption (Masoumi and Dalai, 2020). Thus, the reduction in porosity and specific area of the produced hydrochar might be unsuitable for the application as an admixture for plaster production. For this reason, the hydrodynamic cavitation was performed only on the mixture of SOF and LL. The mixture cavitated at a temperature set point of 60 °C was submitted to the HTC at a process temperature of 250 °C and a residence time of 3 hours to evaluate the effect of the HC on the hydrochar properties. The characteristics of the hydrochars from the HTC process of the mixture of SOF and LL before and after undergoing HC are reported in Table 3.

The hydrodynamic cavitation performed at a temperature set point of 60°C showed significant advantages in terms of hydrochar properties. In detail, HC as pre-treatment of HTC provided higher disintegration and homogenization of the solid/liquid mixture leading to higher carbon and fixed carbon content (+11.37% and +33.68% respectively), lower ash formation (–12.33%) and upgraded DE (+63.91%), lending support for producing hydrochar with raised porosity.

3.2. Central composite face-centered design and analysis

The CCF-CD experimental design was established from the results of the preliminary analysis. In detail, the HTC process was performed by using the mixture of SOF and LL cavitated at a temperature set point of 60°C. The factors and their coded values are shown in Table 4. A total number of 13 tests were carried out, including 4 runs of factorial points, 4 runs of face-centered points, and 5 replicates at the central point useful to evaluate the pure error.

3.2.1. Elemental analysis of hydrochars

Table 5 displays the results of the proximate analysis of hydrochars from the CCF-CD experimental design. The trials were performed in random order for minimising the effects of unexpected variability on the observed responses. The changes in the elemental composition of raw SOF and the obtained hydrochars are also given in the Van Krevelen diagram (Fig. 1), which is a plot of the atomic H/C ratio versus the atomic O/C ratio. The hydrochars had significantly lower H/C and O/C atomic ratios than the raw SOF. This mainly results from the dehydration and decar-boxylation reactions occurring during HTC (Si et al., 2023; Venna et al., 2021). The dehydration and decarboxylation reactions, which reduce the amount of H and O elements and increase the presence of C, were caused by the rise in HTC temperature (Budiman et al., 2022).

Table 2. Characteristics of raw SOF and hydrochars from preliminary tests

Liquid substrate		***LL***	***CF***	***LL***	***CF***	***LL***	***CF***
HTC temperature [°C]		200	200	250	250	270	270
Residence time [h]		1	1	3	3	6	6
Ultimate analysis [wt%$_{daf}$]							
	Raw SOF						
C	22.40	23.60	22.60	30.40	29.20	28.97	24.12
H	3.20	4.42	2.87	2.79	2.36	1.87	2.42
N	1.37	0.88	0.83	1.17	1.27	1.67	1.84
O	17.80	23.56	17.55	11.79	9.15	12.82	14.05
Proximate analysis [wt%$_{db}$]							
Ash	55.82	47.54	56.15	53.85	58.02	47.54	57.57
VM	41.79	46.77	36.73	41.72	36.82	46.77	39.38
FC	2.39	5.69	7.12	4.43	5.16	5.69	3.05
DE [%]	-	38.04	11.32	24.48	16.14	28.45	22.11
MY [%]	-	72.75	88.16	78.28	80.68	72.28	74.72

Note: db: dry basis; daf: dry and ash-free bases

Table 3. Proximate and ultimate analysis of hydrochars before and after HC

Mixture	*Not cavitated*	*Cavitated*
HTC temperature [°C]	250	250
Residence time [h]	3	3
Ultimate analysis [wt%$_{daf}$]		
C	30.40	34.3
H	2.79	3.77
N	1.17	1.44
O	11.79	12.55
Proximate analysis [wt%$_{db}$]		
Ash	53.85	47.94
VM	41.72	45.86
FC	4.43	6.68
DE [%]	24.48	67.86
MY [%]	78.28	37.45

Note: db: dry basis; daf: dry and ash-free bases

Table 4. Independent process variables, range values, and coded levels in experimental design

Independent variables	*Symbols*	*Coded levels*		
		–1	*0*	*1*
HTC temperature [°C]	X_1	220	250	280
Residence time [h]	X_2	1.5	3	4.5

Table 5. Ultimate analysis of hydrochars from CCF-CD experimental design

Run order	*1*	*2*	*3*	*4*	*5*	*6*	*7*	*8*	*9*	*10*	*11*	*12*	*13*
X_1 [°C]	250	250	250	220	250	250	280	220	220	250	280	250	280
X_2 [h]	1.5	3	4.5	3	3	3	4.5	1.5	4.5	3	1.5	3	3
Ultimate analysis [wt%$_{daf}$]													
C	34.70	36.60	37.68	30.13	34.40	35.00	35.13	30.43	33.40	33.20	34.18	33.00	34.85
H	4.03	3.98	4.11	3.61	3.68	4.13	3.48	3.81	3.93	3.67	3.45	3.83	3.40
N	1.32	1.38	1.75	1.04	1.50	1.46	1.24	0.89	0.98	0.89	1.28	1.52	1.15
O	14.19	10.15	12.38	17.58	11.41	12.53	7.76	21.03	15.28	11.65	10.67	12.93	9.70

Note: db: dry basis; daf: dry and ash-free bases

Likewise, the increase in residence time only influenced the O/C ratios, which decreased. While dehydration and decarboxylation are the predominant reaction pathways, demethanation has a negligible influence on the HTC process.

3.2.2. BET analysis of hydrochars

As shown in Fig. 2, the specific surface area of all hydrochars was larger than that of the raw SOF. As the HTC temperature increased from 220 °C to 250 °C, the surface area gradually increased. This might be due to the release of gases from the decomposition of unstable components and the removal of VM during the hydrothermal process, resulting in the formation of open pores and cracks on the surface of the hydrochar (Fu et al., 2022; Wu et al., 2023; Yang et al., 2023).

However, at higher HTC temperatures and long residence times, the surface area decreased, which might be due to the secondary polymerization of soluble intermediates produced during the hydrolysis phase led to the blocking of pores (Magdziarz et al., 2021; Xu et al., 2013; Yang et al., 2023). Even though the values for the surface area were generally low for raw SOF and hydrochars produced at all conditions, ranging from around 7 to 12 m^2/g, they are consistent with previous studies on biomass-derived hydrochars. Low surface area values for hydrochars derived from municipal solid waste, sewage sludge, livestock manure, spent coffee grounds, and macroalgae, have been reported in the literature (Fu et al., 2022; Mlonka-Mędrala et al., 2022; Venkatesan et al., 2022; Wilk et al., 2023; Xu et al., 2013; Yang et al., 2023). Nevertheless, the combination of thermal and chemical or physical activation might explain the surface area increase (Jais et al., 2021; Ogungbenro et al., 2017; Zhang et al., 2021).

3.3. Effect of independent variables

The proximate analysis of hydrochars from the CCF-CD experimental design, together with their respective experimental responses are listed in Table 6. By applying multiple regression analysis to the experimental data, the relationship between the response variables, fixed carbon content (Y_1), deashing efficiency (Y_2), and mass yield (Y_3) of the HTC process, and the input variables, HTC process temperature (X_1) and residence time (X_2), was expressed by second-order polynomial equations with interaction terms. The final models generated in coded factors are shown as described by Eqs. (3-5).

$$Y_1 = -99.18 + 0.8427X_1 + 1.263X_2 - 0.001743X_1X_1 - 0.4149X_2X_2 + 0.00550X_1X_2 \quad (3)$$

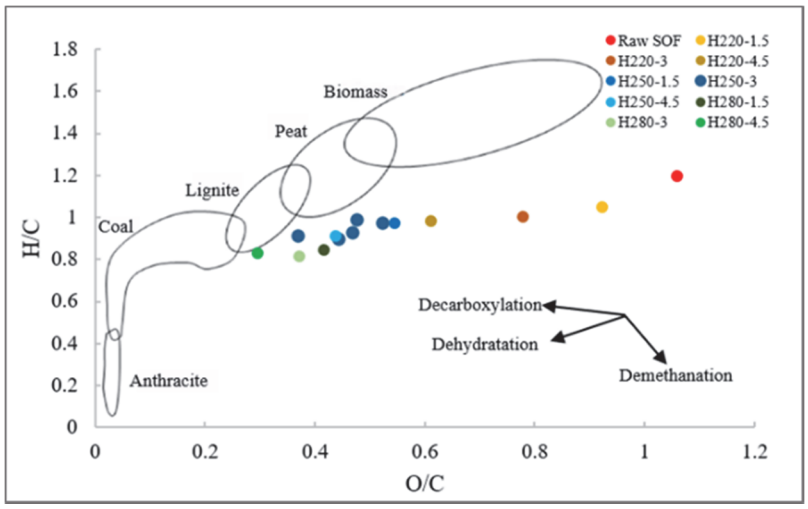

Fig. 1. Van Krevelen diagram for hydrochars under different conditions

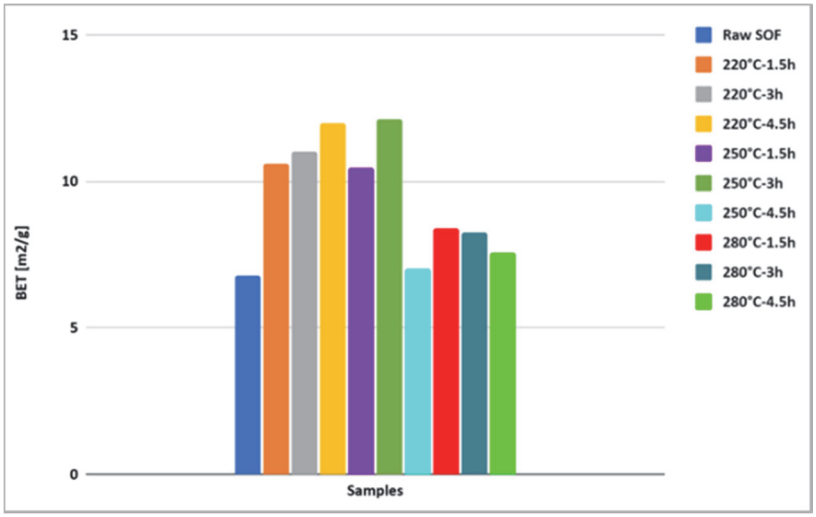

Fig. 2. BET surface area of the hydrochars from CCF-CD experimental design

$$Y_2 = -1635.0 + 13.376X_1 + 3.76X_2 - 0.026446X_1X_1 - 0.534X_2X_2 + 0.0058X_1X_2 \quad (4)$$

$$Y_3 = 1939.2 - 14.675X_1 - 15.60X_2 + 0.02866X_1X_1 + 1.723X_2X_2 + 0.0093X_1X_2 \quad (5)$$

Analysis of variance (ANOVA) was performed for the adequacy and fitness of predicted models and the results are presented in Table 7. The calculated F-values of 70.97, 197.38, and 182.08 for Y_1, Y_2, and Y_3 respectively, demonstrated that the regression models are highly significant ($p < 0.0001$).

There is only a 0.01% chance that these large F-values could occur due to noise, confirming the validity of the predicted model. Furthermore, the adequacy of the model was analyzed by the evaluation of the determination coefficient ($R^2 > 0.95$) and the lack of fit (LOF) test. An R^2 value of 0.9807, 0.9930, and 0.9924 for Y_1, Y_2, and Y_3 respectively, ensured that only 1.93%, 0.7%, and 0.76% of the total variations are not explained by the regression models, validating the precision of the deduced models. Moreover, the values of R^2_{adj} (0.9668, 0.9879, 0.9869) were very high and in reasonable agreement with the R^2 values, confirming that the regression models were highly significant.

The acceptability of the quadratic models was also verified by the lack of fit (LOF) test. A p-value higher than 0.05 means that LOF is insignificant due to relative pure error. Thus, the lack of fit p-values (0.265, 0.093, and 0.120 for each model) confirms that the models can be effectively employed for the prediction.

3.3.1. Effect on fixed carbon content

The influence of the independent variables on the responses and their interactions were evaluated by plotting response surface graphs and contour plots. Fig. 3 shows the effects of process temperature and residence time on fixed carbon content. The FC content increased with the increase in process temperature from 220 to 250°C and then decreased at the higher process temperature of 280°C.

Table 6. Proximate analysis of hydrochars from CCF-CD experimental design

Run order	***1***	***2***	***3***	***4***	***5***	***6***	***7***	***8***	***9***	***10***	***11***	***12***	***13***
X_1 [°C]	250	250	250	220	250	250	280	220	220	250	280	250	280
X_2 [h]	1.5	3	4.5	3	3	3	4.5	1.5	4.5	3	1.5	3	3
Proximate analysis [wt%$_{db}$]													
Ash	45.76	47.89	44.09	47.64	49.01	46.88	52.39	43.84	46.41	50.58	50.44	48.71	50.90
VM	48.78	45.59	50.08	46.95	44.12	46.17	43.13	51.47	48.91	42.60	46.06	44.34	44.49
FC (Y_1)	5.46	6.52	5.83	5.41	6.87	6.95	4.48	4.69	4.68	6.82	3.50	6.95	4.61
DE (Y_2) [%]	60.45	67.51	70.17	37.86	65.63	67.98	49.78	35.10	38.77	67.68	45.06	66.88	47.56
MY (Y_3) [%]	47.73	37.47	37.37	72.04	38.73	37.72	52.94	81.76	72.87	35.29	60.16	37.55	56.90

Note: db: dry basis; daf: dry and ash-free bases

Table 7. ANOVA of response surface quadratic models

Source	***DF***	***F-Value***	***Prob > F***
Fixed carbon content			
Model	5	70.97	< 0.0001
X_1	1	18.06	0.004
X_2	1	6.76	0.035
X_1X_1	1	153.47	< 0.0001
X_2X_2	1	54.36	< 0.0001
X_1X_2	1	5.53	0.051
Lack-of-Fit	3	1.94	0.265
$R^2 = 0.9807$; $R^2_{adj} = 0.9668$			
Deashing efficiency			
Model	5	197.38	< 0.0001
X_1	1	73.08	< 0.0001
X_2	1	25.48	0.001
X_1X_1	1	729.38	< 0.0001
X_2X_2	1	1.86	0.215
X_1X_2	1	0.13	0.731
Lack-of-Fit	3	4.42	0.093
$R^2 = 0.9930$; $R^2_{adj} = 0.9879$			
Mass yield			
Model	5	182.08	< 0.0001
X_1	1	157.31	< 0.0001
X_2	1	34.32	0.001
X_1X_1	1	540.20	< 0.0001
X_2X_2	1	12.20	0.010
X_1X_2	1	0.20	0.664
Lack-of-Fit	3	3.68	0.120
$R^2 = 0.9924$; $R^2_{adj} = 0.9869$			

This result is in agreement with previous studies (Zhang et al., 2016). Moreover, according to the F-values and p-values of Table 7, it can be noted that for the FC content X_1, X_2, X_1X_1, and X_2X_2 are significant model terms because their p-values were higher than 0.05. From the F-values, the process temperature (X_1) had a slightly greater effect on the FC content rather than residence time (X_2). Therefore, the positive signs of X_1 and X_2 in the Eq. (3) indicate synergistic effects on the FC. However, the negative signs of X_1X_1 and X_2X_2 provide antagonistic effects on the response which make the FC increase up to a certain threshold with increasing HTC temperature and residence time after which it decreases.

3.3.2. Effect on dashing efficiency

A similar trend obtained for the FC was found for the deashing efficiency (Fig. 4). The proximate analysis of Table 6 shows that the DE increased from 35.10% up to 70.17% with the increase of process temperature and residence time from 220°C and 1.5h to 250°C and 4.5h and then decreasing up to 45.06% at 280°C and 1.5h. Similar findings were observed in literature studies (Mohammed et al., 2020; Nakason et al., 2018; Tahmid Islam et al., 2023). This was expected to be due to the fact that the ash can be leached into the liquid fraction during HTC and its increase may be caused by the condensation and reprecipitation of some inorganics on the hydrochar surface after a long residence time at high temperatures. Furthermore, the F-values and p-values of Table 7 highlighted how X_1, X_2, and X_1X_1 are significant model terms. Likewise, for FC content, the F-values of process temperature (X_1) had a slightly greater effect on the DE rather than residence time (X_2), while the quadratic effect of process temperature (X_1X_1) showed a higher impact. However, an important result from the ANOVA analysis is that the

residence time had no significant quadratic and interactive effects on the dashing efficiency.

3.3.3. Effect on mass yield

The effect of the independent variables on hydrochars mass yield is shown in Fig. 5. By considering each process temperature, the increase in residence time determined a slight decrease in MY. On the other hand, the hydrochar yield decreased by a mean of 46% points from 220°C to 250°C and increased again by a mean of 40% points from 250°C to 280°C. The decrease in the yield as a function of temperature and residence time might be due to the higher carbonization degree, which led to a higher degree of material decomposition, fragmentation, and solubilization (Melo et al., 2017; Roslan et al., 2023; Wilk et al., 2023). Furthermore, by raising the HTC temperature from 250°C to 280°C the formation of secondary char by polymerization reactions of small molecules in the liquid phase and recondensation into the char phase made the mass yield increase (Surup et al., 2020).

The influence of the independent variables is confirmed by the ANOVA analysis, as reported in Table 7. All linear and quadratic terms were significant. In detail, having the highest F-value for both linear and quadratic coefficients, the process temperature affected most significantly the MY and might be considered the main controlling factor of the HTC process. Furthermore, the positive coefficients of the quadratic terms X_1X_1 and X_2X_2 denoted that there is a possible point of deflexion after which the independent variables have a negative or positive effect on the MY.

3.4. Determination and validation of optimum conditions

Since the aim of this work is the preliminary investigation of the possible use of hydrochar as an admixture for the production of a sustainable plaster as carbon-capture, thermal insulation, moisture absorption, and acoustic insulation material, the FC, DE, and MY were chosen as response variables to obtain the optimum HTC process conditions at which they are maximized. By using hydrochar as an admixture, plasters and other building materials might benefit from its low thermal conductivity, high surface area, and porous nature.

These properties work together to enhance the plaster thermal insulation by disrupting the thermal bridging, rendering the heat propagation routes multi-directional and hindering the effect of unidirectional heat propagation, thus reducing the propagation of heat flow (Cuthbertson et al., 2019; Zhang et al., 2022).

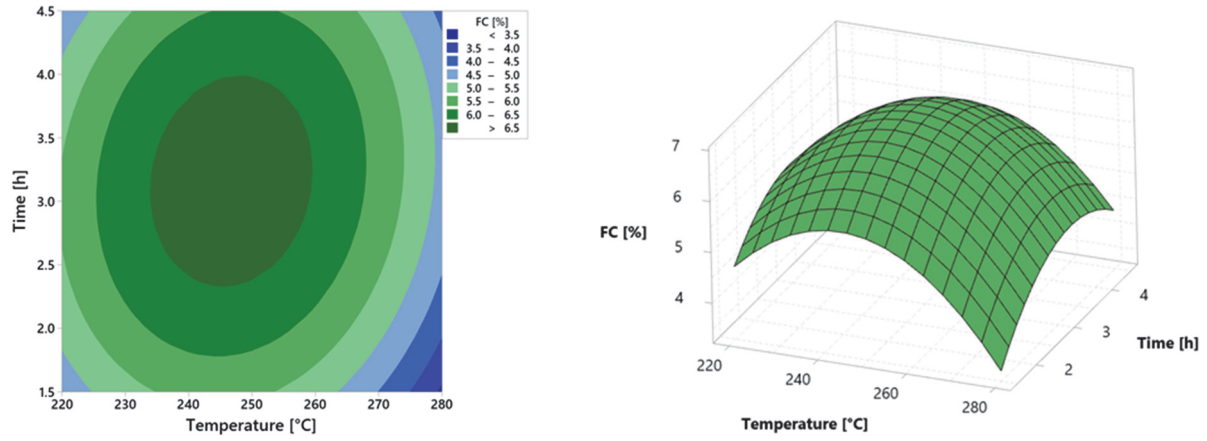

Fig. 3. Contour and surface plots of the fixed carbon content vs the independent variables (temperature and time)

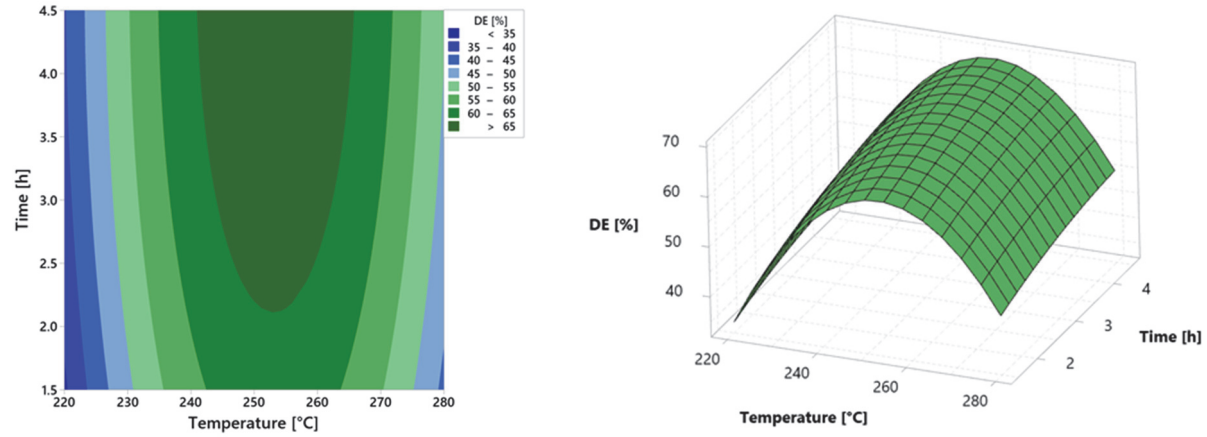

Fig. 4. Contour and surface plots of deashing efficiency vs the independent variables (temperature and time)

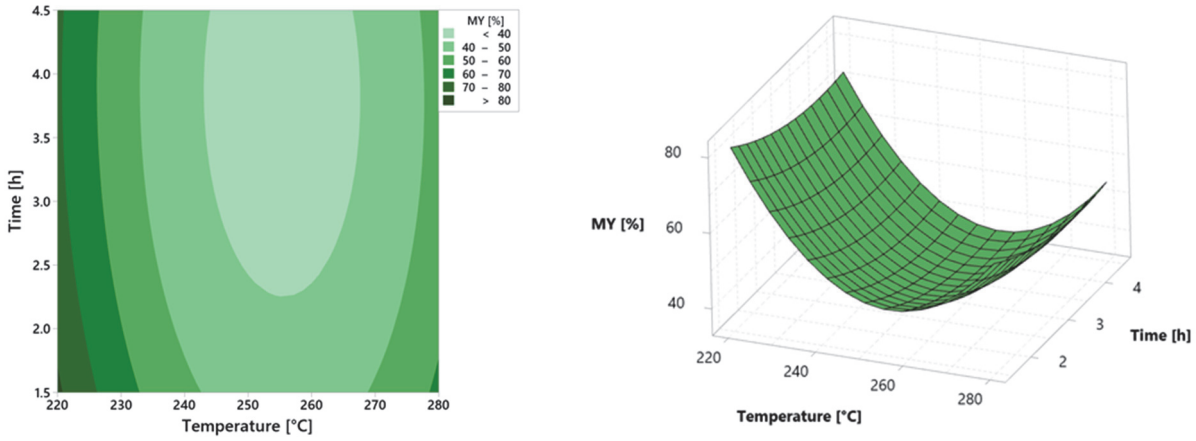

Fig. 5. Contour and surface plots of mass yield vs. the independent variables (temperature and time)

Additionally, hydrochar could increase the ability of the plaster to absorb sound, as sound waves would disperse and converted into heat through refraction within the increased porosity and interconnected pore networks of the admixture (Mota-Panizio et al., 2023; Rojas et al., 2019). Furthermore, a high surface area is favorable for the formation of a suitable pore structure for CO_2 uptake, which is subsequently mineralized into stable carbonates after being released into the plaster matrix, and moisture adsorption, which can help to regulate the relative humidity (Cuthbertson et al., 2019; Deepak et al., 2023; Gupta et al., 2022; Roychand et al., 2023; Zhang et al., 2022). These considerations are strictly related to the chosen response variables. The high ash content in the SOF may clog the pores, resulting in a decrease in specific surface area during the hydrothermal carbonization process (Gao et al., 2022). On the other hand, with the increase of FC the surface area of hydrochar generally shows a regular increase (Kahandawa Arachchi et al., 2021; Tu et al., 2021). This is because of the dehydration, decarboxylation, and devolatilization reactions, which increase the carbon content and open these clogged pores (Wang et al., 2022b). Furthermore, a higher MY could lead to greater efficiency in the production process, reducing production costs and increasing the economic viability of hydrochar in large-scale industrial production (Hussin et al., 2023; Yao et al., 2023). Thus, the deashing effect of the HTC process, the fixed carbon and the mass yield, should be maximised to enhance the characteristics of the plaster. However, the optimization of all responses under the same operative conditions is difficult because their intervals of variation are different. For this reason, the multi-response optimization was carried out by the desirability function approach. Composite desirability evaluates how the settings optimize a set of responses overall (Barbanera et al., 2021). In this study, equal weightage was given for all responses (FC, DE and MY) and an importance parameter equal to 1 were assumed. As can be noted in Fig. 6 the composite desirability (D) of the optimization was 56.87%, indicating that it is challenging to optimize all the response variables simultaneously. In particular, the maximum fixed carbon content, deashing efficiency and mass yield was found to be 6.34%, 54.73% and 53.81% respectively at an optimal parametric combination of a process temperature of 232°C and a residence time of 2.65h.

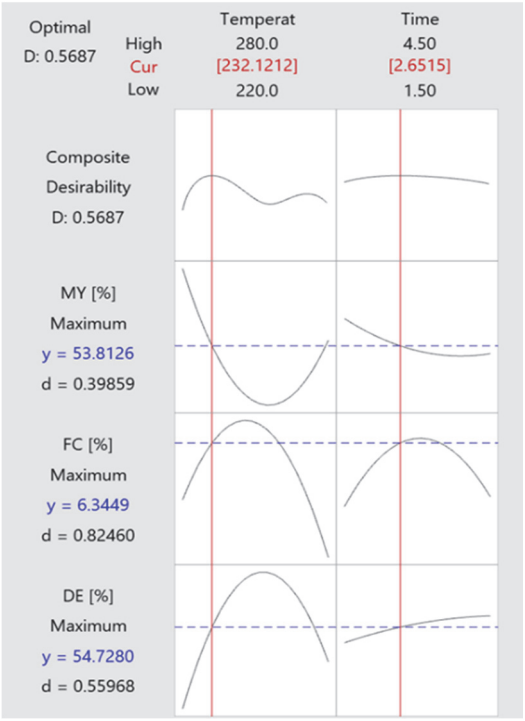

Fig. 6. Optimization plots of the operating variables

To consolidate the results of the model, a hydrothermal carbonization treatment of the cavitated mixture of SOF and LL was performed under the optimized conditions. Experiments were performed in triplicate and the values of the response variables are reported in Table 8. Results confirm the suitability of the developed quadratic models because the experimental findings are in close agreement with the predicted values within a < 3% error (Table 8).

Table 8. Physicochemical characterization of hydrochar and response variables at the optimal HTC conditions

Analysis	*Measured*	*Predicted*	*Deviation [%]*
FC (Y_1) [%]	6.17	6.34	–2.64
DE (Y_2) [%]	53.87	54.73	–1.58
MY (Y_3) [%]	54.26	53.81	0.84

Note: db: dry basis; daf: dry and ash-free bases

4. Conclusions

In this work, the hydrothermal carbonization of the stabilized organic fraction of municipal solid waste was performed at several process conditions by using landfill leachate as a liquid substrate. Also, the hydrodynamic cavitation was confirmed as a valid pretreatment to enhance both the homogenization of the slurry, avoiding incurring pumpability problems at an industrial scale, and the hydrochar characteristics. Furthermore, the Central Composite Face-Centered Design together with the Response Surface Model proved to be very useful in determining the influence of independent variables (process temperature and residence time) on the response variables (FC, DE, and MY), thus the optimal conditions for the HTC process of the cavitated mixture of SOF and LL. In detail, HTC temperature has the most influence on the physicochemical properties of hydrochar while the effects of residence time are less significant.

However, analysis of variance showed high R^2 values, indicating a good fit of the regression models to the experimental data. The optimum conditions for the HTC process found at 232°C and 2.65 h resulted in a fixed carbon content of 6.17%, a deashing efficiency of 53.87%, and a mass yield of 54.26%. Under the optimized conditions obtained from Derringer's desired function methodology, the experimental values are in close agreement with the predicted ones.

Acknowledgements

The authors would like to acknowledge the project ECOPLASTER (J83C22000290001)- Biostabilized for Ecosustainable Building - funded by the Ministry of Environment and Energetic Security. This research was supported by the project ECS00000024 "Ecosistemi dell'Innovazione" - Rome Technopole of the Italian Ministry of University and Research, public call n. 3277, PNRR—Mission 4, Component 2, Investment 1.5, financed by the European Union, Next GenerationEU.

References

Barbanera M., Cardarelli A., Carota E., Castellini M., Giannoni T., Ubertini S., (2021), Valorization of winery and distillery by-products by hydrothermal carbonization, *Scientific Reports*, **11**, 23973, https://doi.org/10.1038/s41598-021-03501-7.

Barbanera M., Pelosi C., Taddei A.R., Cotana F., (2018), Optimization of bio-oil production from solid digestate by microwave-assisted liquefaction, *Energy Conversion and Management*, **171**, 1263-1272.

Basso D., Weiss-Hortala E., Patuzzi F., Castello D., Baratieri M., Fiori L., (2015), Hydrothermal carbonization of off-specification compost: A byproduct of the organic municipal solid waste treatment, *Bioresource Technology*, **182**, 217-224.

Başakçılardan Kabakcı S., Baran S.S., (2019), Hydrothermal carbonization of various lignocellulosics: Fuel characteristics of hydrochars and surface characteristics of activated hydrochars, Waste Management, **100**, 259-268.

Budiman I., Subyakto Syafitri U.D., Widyaningrum B.A., Marlina R., Triastuti, Widodo E., (2022), Characteristics optimization of empty fruit bunches chars using central composite design, *Biomass Conversion and Biorefinery*, https://doi.org/10.1007/s13399-022-02892-5.

Buratti C., Barbanera M., Lascaro E., Cotana F., (2018), Optimization of torrefaction conditions of coffee industry residues using desirability function approach, *Waste Management*, **73**, 523-534.

Castro J.D.S., Assemany P.P., Carneiro A.C.D.O., Ferreira J., De Jesus Junior M.M., Rodrigues F.D.A., Calijuri M.L., (2021), Hydrothermal carbonization of microalgae biomass produced in agro-industrial effluent: Products, characterization and applications, *Science of The Total Environment*, **768**, 144480, https://doi.org/10.1016/j.scitotenv.2020.144480

Cavali M., Libardi Junior N., Mohedano R.D.A., Belli Filho P., Da Costa R.H.R., De Castilhos Junior A.B., (2022), Biochar and hydrochar in the context of anaerobic digestion for a circular approach: An overview, *Science of the Total Environment*, **822**, 153614, https://doi.org/10.1016/j.scitotenv.2022.153614

Chen C., Liang W., Fan F., Wang C., (2021), The effect of temperature on the properties of hydrochars obtained by hydrothermal carbonization of waste Camellia oleifera shells, *ACS Omega*, **6**, 16546–16552.

Cuthbertson D., Berardi U., Briens C., Berruti F., (2019), Biochar from residual biomass as a concrete filler for improved thermal and acoustic properties, *Biomass and Bioenergy*, **120**, 77–83.

Danso-Boateng E., Ross A.B., Mariner T., Hammerton J., Fitzsimmons M., (2022), Hydrochars produced by hydrothermal carbonisation of seaweed, coconut shell and oak: Effect of processing temperature on physicochemical adsorbent characteristics, *SN Applied Sciences*, **4**, 203, https://doi.org/10.1007/s42452-022-05085-x

Deepak K.R., Mohan S., Dinesha P., Balasubramanian R., (2023), CO_2 uptake by activated hydrochar derived from orange peel (Citrus reticulata): Influence of carbonization temperature, *Journal of Environmental Management*, **342**, 118350, https://doi.org/10.1016/j.jenvman.2023.118350

Derringer G., Suich R., (1980), Simultaneous Optimization of Several Response Variables, *Journal of Quality Technology*, **12**, 214-219.

Djandja O.S., Liew R.K., Liu C., Liang J., Yuan H., He W., Feng Y., Lougou B.G., Duan P.-G., Lu X., Kang S., (2023), Catalytic hydrothermal carbonization of wet organic solid waste: A review, *Science of the Total Environment*, **873**, 162119,

https://doi.org/10.1016/j.scitotenv.2023.162119

Ercan B., Alper K., Ucar S., Karagoz S., (2023), Comparative studies of hydrochars and biochars produced from lignocellulosic biomass via hydrothermal carbonization, torrefaction and pyrolysis. *Journal of the Energy Institute*, **109**, 101298, https://doi.org/10.1016/j.joei.2023.101298

Eurostat, (2023), Overview – Waste - Eurostat, On line at: Https://ec.europa.eu/eurostat/web/waste

Fu H., Wang B., Wang H., Liu H., Xie H., Han L., Wang N., Sun X., Feng Y., Xue L., (2022), Assessment of livestock manure-derived hydrochar as cleaner products: Insights into basic properties, nutrient composition, and heavy metal content, *Journal of Cleaner Production*, **330**, 129820, https://doi.org/10.1016/j.jclepro.2021.129820

Gao Q., Ni L., He Y., Hou Y., Hu W., Liu Z., (2022), Effect of hydrothermal pretreatment on deashing and pyrolysis characteristics of bamboo shoot shells, *Energy*, 247, 123510, https://doi.org/10.1016/j.energy.2022.123510

González-Arias J., De La Rubia M.A., Sánchez M.E., Gómez X., Cara-Jiménez J., Martínez E.J., (2023), Treatment of hydrothermal carbonization process water by electrochemical oxidation: Assessment of process performance, *Environmental Research*, **216**, 114773, https://doi.org/10.1016/j.envres.2022.114773

Gupta S., Kua H.W., (2017), Factors determining the potential of biochar as a carbon capturing and sequestering construction material: critical review, *Journal of Materials in Civil Engineering*, **29**, 04017086, https://doi.org/10.1061/(ASCE)MT.1943-5533.0001924.

Gupta S., Kashani A., Mahmood A.H., (2022), Carbon sequestration in engineered lightweight foamed mortar – Effect on rheology, mechanical and durability properties, *Construction and Building Materials*, **322**, 126383, https://doi.org/10.1016/j.conbuildmat.2022.126383

Hussin F., Hazani N.N., Khalil M., Aroua M.K., (2023), Environmental life cycle assessment of biomass conversion using hydrothermal technology: A review, *Fuel Processing Technology*, **246**, 107747, https://doi.org/10.1016/j.fuproc.2023.107747

Ischia G., Fiori L., Gao L., Goldfarb J.L., (2021), Valorizing municipal solid waste via integrating hydrothermal carbonization and downstream extraction for biofuel production, *Journal of Cleaner Production*, **289**, 125781, https://doi.org/10.1016/j.jclepro.2021.125781.

Ipiales R.P., de la Rubia M.A., Diaz E., Mohedano A.F., Rodriguez J.J., (2021), Integration of hydrothermal carbonization and anaerobic digestion for energy recovery of biomass waste: An overview, *Energy Fuels*, **35**, 17032-17050.

ISPRA, (2022), Municipal Waste Report 2022 Edition (in Italian), On line at: Https://www.isprambiente.gov.it/it/pubblicazioni/rapporti/rapporto-rifiuti-urbani-edizione-2022

Jabeen S., Gao X., Hayashi J., Altarawneh M., Dlugogorski B.Z., (2023), Effects of product recovery methods on the yields and properties of hydrochars from hydrothermal carbonization of algal biomass, *Fuel*, **332**, 126029, https://doi.org/10.1016/j.fuel.2022.126029

Jais F.M., Chee C.Y., Ismail Z., Ibrahim S., (2021), Experimental design via NaOH activation process and statistical analysis for activated sugarcane bagasse hydrochar for removal of dye and antibiotic, *Journal of Environmental Chemical Engineering*, **9**, 104829, https://doi.org/10.1016/j.jece.2020.104829

Kahandawa Arachchi K.A.D.Y.T., Selvaratnam A., Gamage J.C.P.H., De Silva G.I.P., (2021), Green composite plaster with modified morphology for enhanced thermal comfort in buildings, *Case Studies in Construction Materials*, **15**, e00611, https://doi.org/10.1016/j.cscm.2021.e00611.

Khan T.A., Saud A.S., Jamari S.S., Rahim M.H.A., Park J.-W., Kim H.-J., (2019), Hydrothermal carbonization of lignocellulosic biomass for carbon rich material preparation: A review, *Biomass and Bioenergy*, **130**, 105384, https://doi.org/10.1016/j.biombioe.2019.105384

Lanfranchi A., Tassinato G., Valentino F., Martinez G.A., Jones E., Gioia C., Bertin L., Cavinato C., (2022), Hydrodynamic cavitation pre-treatment of urban waste: Integration with acidogenic fermentation, PHAs synthesis and anaerobic digestion processes, *Chemosphere*, **301**, 134624, https://doi.org/10.1016/j.chemosphere.2022.134624.

Langone M., Dasso D., (2020), Process waters from hydrothermal carbonization of sludge: characteristics and possible valorization pathways, International *Journal of Environmental Research and Public Health*, **17**, 6618, https://doi.org/10.3390/ijerph17186618

Libra J.A., Ro K.S., Kammann C., Funke A., Berge N.D., Neubauer Y., Titirici M.-M., Fühner C., Bens O., Kern J., Emmerich K.-H., (2011), Hydrothermal carbonization of biomass residuals: a comparative review of the chemistry, processes and applications of wet and dry pyrolysis, *Biofuels*, **2**, 89-124.

Luo X., Huang Z., Lin J., Li X., Qiu J., Liu J., Mao X., (2020), Hydrothermal carbonization of sewage sludge and in-situ preparation of hydrochar/MgAl-layered double hydroxides composites for adsorption of Pb(II), *Journal of Cleaner Production*, **258**, 120991, https://doi.org/10.1016/j.jclepro.2020.120991

Magdziarz A., Mlonka-Mędrala A., Sieradzka M., Aragon-Briceño C., Pożarlik A., Bramer E.A., Brem G., Niedzwiecki L., Pawlak-Kruczek H., (2021), Multiphase analysis of hydrochars obtained by anaerobic digestion of municipal solid waste organic fraction, *Renewable Energy,* **175**, 108-118.

Masoumi S., Dalai A.K., (2020), Optimized production and characterization of highly porous activated carbon from algal-derived hydrochar, *Journal of Cleaner Production*, **263**, 121427, https://doi.org/10.1016/j.jclepro.2020.121427.

Melo C.A., Junior F.H.S., Bisinoti M.C., Moreira A.B., Ferreira O.P., (2017), Transforming sugarcane bagasse and vinasse wastes into hydrochar in the presence of phosphoric acid: an evaluation of nutrient contents and structural properties, *Waste and Biomass Valorization*, **8**, 1139-1151.

Mendecka B., Lombardi L., Micali F., De Risi A., (2020), Energy recovery from olive pomace by hydrothermal carbonization on hypothetical industrial scale: A LCA perspective, *Waste and Biomass Valorization*, **11**, 5503–5519.

Mlonka-Mędrala M., Sieradzka M., Magdziarz A., (2022), Thermal upgrading of hydrochar from anaerobic digestion of municipal solid waste organic fraction, *Fuel,* **324**, 124435, https://doi.org/10.1016/j.fuel.2022.124435

Mohammadi, A., Venkatesh, G., Sandberg, M., Eskandari, S., Joseph, S., & Granström, K. (2020). A comprehensive environmental Life Cycle Assessment of the use of hydrochar pellets in combined heat and power plants, *Sustainability*, **12**, 9026,

https://doi.org/10.3390/su12219026
Mohammed I.S., Na R., Kushima K., Shimizu N., (2020), Investigating the effect of processing parameters on the products of hydrothermal carbonization of corn stover, *Sustainability*, **12**, 5100, https://doi.org/10.3390/su12125100.
Mota-Panizio R., Carmo-Calado L., Assis A.C., Matos V., Hermoso-Orzáez M.J., Romano P., Gonçalves M., Brito P., (2023), Properties and uses of biochars incorporated into mortars, *Environments*, **10**, 47, https://doi.org/10.3390/environments10030047
Mrad R., Chehab G., (2019), Mechanical and microstructure properties of biochar-based mortar: an internal curing agent for PCC, *Sustainability*, **11**, 2491, https://doi.org/10.3390/su11092491.
Nagarajan S., Ranade V.V., (2021), Valorizing Waste Biomass via Hydrodynamic Cavitation and Anaerobic Digestion, *Industrial and Engineering Chemistry Research*, **60**, 16577-16598.
Nakason K., Panyapinyopol B., Kanokkantapong V., Viriya-empikul N., Kraithong W., Pavasant P., (2018), Characteristics of hydrochar and liquid fraction from hydrothermal carbonization of cassava rhizome, *Journal of the Energy Institute*, **91**, 184-193.
Navaratnam S., Wijaya H., Rajeev P., Mendis P., Nguyen K., (2021), Residual stress-strain relationship for the biochar-based mortar after exposure to elevated temperature, *Case Studies in Construction Materials*, **14**, e00540, https://doi.org/10.1016/j.cscm.2021.e00540.
Nawaz A., Kumar P., (2023), Impact of temperature severity on hydrothermal carbonization: Fuel properties, kinetic and thermodynamic parameters, *Fuel*, 336, 127166, https://doi.org/10.1016/j.fuel.2022.127166
Naveen B.P., Mahapatra D.M., Sitharam T.G., Sivapullaiah P.V., Ramachandra T.V., (2017), Physico-chemical and biological characterization of urban municipal landfill leachate, *Environmental Pollution*, **220**, 1-12.
Ogungbenro A.E., Quang D.V., Al-Ali K., Abu-Zahra M.R.M., (2017), Activated carbon from date seeds for CO_2 capture applications, *Energy Procedia*, 114, 2313-2321.
Periyavaram S.R., Uppala L., Sivaprakash S., Reddy P.H.P., (2023), Thermal behaviour of hydrochar derived from hydrothermal carbonization of food waste using leachate as moisture source: Kinetic and thermodynamic analysis, *Bioresource Technology*, **373**, 128734, https://doi.org/10.1016/j.biortech.2023.128734.
Rojas C., Cea M., Iriarte A., Valdes G., Navia R., Cardenas-R, J.P., (2019), Thermal insulation materials based on agricultural residual wheat straw and corn husk biomass, for application in sustainable buildings, *Sustainable Materials and Technologies*, **20**, e00102, https://doi.org/10.1016/j.susmat.2019.e00102
Roman F.F., Diaz de Tuesta J.L., Praça P., Silva A.M.T., Faria J.L., Gomes H.T., (2021), Hydrochars from compost derived from municipal solid waste: Production process optimization and catalytic applications, *Journal of Environmental Chemical Engineering*, **9**, 104888, https://doi.org/10.1016/j.jece.2020.104888
Roslan S.Z., Zainudin S.F., Mohd Aris A., Chin K.B., Musa M., Mohamad Daud A.R., Syed Hassan S.S.A., (2023), Hydrothermal carbonization of sewage sludge into solid biofuel: influences of process conditions on the energetic properties of hydrochar, *Energies*, **16**, 2483, https://doi.org/10.3390/en16052483.
Roychand R., Li J., Kilmartin-Lynch S., Saberian M., Zhu J., Youssf O., Ngo T., (2023), Carbon sequestration from waste and carbon dioxide mineralisation in concrete – A stronger, sustainable and eco-friendly solution to support circular economy, *Construction and Building Materials*, **379**, 131221, https://doi.org/10.1016/j.conbuildmat.2023.131221
Sharma H.B., Sarmah A.K., Dubey B., (2020), Hydrothermal carbonization of renewable waste biomass for solid biofuel production: A discussion on process mechanism, the influence of process parameters, environmental performance and fuel properties of hydrochar, *Renewable and Sustainable Energy Reviews*, **123**, 109761, https://doi.org/10.1016/j.rser.2020.109761
Si H., Zhao C., Wang B., Liang X., Gao M., Jiang Z., Yu H., Yang Y., Gu Z., Ogino K., Chen X., (2023), Liquid-solid ratio during hydrothermal carbonization affects hydrochar application potential in soil: Based on characteristics comparison and economic benefit analysis, *Journal of Environmental Management,* **335**, 117567, https://doi.org/10.1016/j.jenvman.2023.117567
Śliz M., Tuci F., Czerwińska K., Fabrizi S., Lombardi L., Wilk M., (2022), Hydrothermal carbonization of the wet fraction from mixed municipal solid waste: Hydrochar characteristics and energy balance, *Waste Management*, **151**, 39-48.
Soldo Cavitators, (2023), Emulsification with Soldo Cavitators Technology, On line at: Https://soldocavitators.com/omogeneizzazione-industriale/#
Srikanth G., Fernando A., Selvaranjan K., Gamage J.C.P.H., Ekanayake L., (2022), Development of a plastering mortar using waste bagasse and rice husk ashes with sound mechanical and thermal properties, *Case Studies in Construction Materials*, **16**, e00956, https://doi.org/10.1016/j.cscm.2022.e00956.
Surup G.R., Leahy J.J., Timko M.T., Trubetskaya A., (2020), Hydrothermal carbonization of olive wastes to produce renewable, binder-free pellets for use as metallurgical reducing agents, *Renewable Energy*, **155**, 347-357.
Tahmid Islam M., Klinger J.L., Toufiq Reza M., (2023), Evaluating combustion characteristics and combustion kinetics of corn stover-derived hydrochars by cone calorimeter, *Chemical Engineering Journal*, **452**, 139419, https://doi.org/10.1016/j.cej.2022.139419.
Tripathi A.D., Mishra P.K., Darani K.K., Agarwal A., Paul V., (2022), Hydrothermal treatment of lignocellulose waste for the production of polyhydroxyalkanoates copolymer with potential application in food packaging, *Trends in Food Science & Technology*, **123**, 233–250.
Tu R., Sun Y., Wu Y., Fan X., Cheng S., Jiang E., Xu X., (2021), A new index for hydrochar based on fixed carbon content to predict its structural properties and thermal behaviour, *Energy*, **229**, 120572, https://doi.org/10.1016/j.energy.2021.120572
Venna S., Sharma H.B., Reddy P.H.P., Chowdhury S., Dubey B.K., (2021), Landfill leachate as an alternative moisture source for hydrothermal carbonization of municipal solid wastes to solid biofuels, *Bioresource Technology*, **320**, 124410, https://doi.org/10.1016/j.biortech.2020.124410.
Venkatesan S., Baloch H.A., Jamro I.A., Rafique R., (2022), Evaluation of the production of hydrochar from spent coffee grounds under different operating conditions,

Journal of Water Process Engineering, **49**, 103037, https://doi.org/10.1016/j.jwpe.2022.103037

Villamil J.A., De La Rubia M.A., Diaz E., Mohedano A.F., (2020), *Technologies for Wastewater Sludge Utilization and Energy Production: Hydrothermal Carbonization of Lignocellulosic Biomass and Sewage Sludge*, In: *Wastewater Treatment Residues as Resources for Biorefinery Products and Biofuels*, Olivares J.A., Melero J.A., Puyol D., Dufour J. (Eds.), Elsevier, Amsterdam, 133–153.

Wang X., Li Z., Cheng Y., Yao H., Li H., You X., Zhang C., Li Y., (2022a), Wheat straw hydrochar induced negative priming effect on carbon decomposition in a coastal soil, *iMeta*, **2**, e134, https://doi.org/10.1002/imt2.134

Wang Q., Wu S., Cui D., Zhou H., Wu D., Pan S., Xu F., Wang Z., (2022b), Co-hydrothermal carbonization of organic solid wastes to hydrochar as potential fuel: A review, *Science of The Total Environment*, **850**, 158034, https://doi.org/10.1016/j.scitotenv.2022.158034

Wilk M., Magdziarz A., Kalemba-Rec I., Szymańska-Chargot M., (2020), Upgrading of green waste into carbon-rich solid biofuel by hydrothermal carbonization: The effect of process parameters on hydrochar derived from acacia, *Energy*, **202**, 117717, https://doi.org/10.1016/j.energy.2020.117717

Wilk M., Czerwińska K., Śliz M., Imbierowicz M., (2023), Hydrothermal carbonization of sewage sludge: Hydrochar properties and processing water treatment by distillation and wet oxidation, *Energy Reports*, **9**, 39–58, https://doi.org/10.1016/j.egyr.2023.03.092

Wu S., Wang Q., Cui D., Wu D., Bai J., Qin H., Xu F., Wang Z., (2023), Insights into the chemical structure evolution and carbonisation mechanism of biomass during hydrothermal treatment, *Journal of the Energy Institute*, 108, 101257, https://doi.org/10.1016/j.joei.2023.101257

Xu Q., Qian Q., Quek A., Ai N., Zeng G., Wang J., (2013), Hydrothermal carbonization of macroalgae and the effects of experimental parameters on the properties of hydrochars, *ACS Sustainable Chemical Engineering*, **1**, 1092-1101.

Yang X., Wang B., Guo Y., Yang F., Cheng F., (2023), Insights into the structure evolution of sewage sludge during hydrothermal carbonization under different temperatures, *Journal of Analytical and Applied Pyrolysis*, **169**, 105839, https://doi.org/10.1016/j.jaap.2022.105839

Yao F., Ye G., Peng W., Zhao G., Wang X., Wang Y., Zhu W., Jiao Y., Huang H., Ye D., (2023), Preparation of activated biochar with adjustable pore structure by hydrothermal carbonization for efficient adsorption of VOCs and its practical application prospects, *Journal of Environmental Chemical Engineering*, **11**, 109611, https://doi.org/10.1016/j.jece.2023.109611

Zhang S., Chen T., Li W., Dong Q., Xiong Y., (2016), Physicochemical properties and combustion behavior of duckweed during wet torrefaction, *Bioresource Technology*, **218**, 1157-1162.

Zhang Z., Li Y., Ding L., Yu J., Zhou Q., Kong Y., Ma J., (2021), Novel sodium bicarbonate activation of cassava ethanol sludge derived biochar for removing tetracycline from aqueous solution: Performance assessment and mechanism insight, *Bioresource Technology,* **330**, 124949, https://doi.org/10.1016/j.biortech.2021.124949

Zhang Y., He M., Wang L., Yan J., Ma B., Zhu X., Ok Y.S., Mechtcherine V., Tsang D.C.W., (2022), Biochar as construction materials for achieving carbon neutrality, *Biochar*, **4**, 59, https://doi.org/10.1007/s42773-022-00182-x

Zhang Q., Wang B., Feng Y., Feng Y., Li J., Ding S., He H., Xie H., (2023), Process water from hydrothermal carbonization: The impacts on the aquatic dissolved organic matter feature and microbial network at the soil-water interface, *Journal of Cleaner Production*, **397**, 136486, https://doi.org/10.1016/j.jclepro.2023.136486